Dynamic Behavior of Rod Photoreceptor Disks

Chunhe Chen, Yunhai Jiang, and Yiannis Koutalos
Department of Physiology and Biophysics, University of Colorado Health Sciences Center, Denver, Colorado 80262 USA

ABSTRACT Eukaryotic cells use membrane organelles, like the endoplasmic reticulum or the Golgi, to carry out different functions. Vertebrate rod photoreceptors use hundreds of membrane sacs (the disks) for the detection of light. We have used fluorescent tracers and single cell imaging to study the properties of rod photoreceptor disks. Labeling of intact rod photoreceptors with membrane markers and polar tracers revealed communication between intradiskal and extracellular space. Internalized tracers moved along the length of the rod outer segment, indicating communication between the disks as well. This communication involved the exchange of both membrane and aqueous phase and had a time constant in the order of minutes. The communication pathway uses ~2% of the available membrane disk area and does not allow the passage of molecules larger than 10 kDa. It was possible to load the intradiskal space with fluorescent Ca^{2+} and pH dyes, which reported an intradiskal Ca^{2+} concentration in the order of 1 μM and an acidic pH 6.5, both of them significantly different than intracellular and extracellular Ca^{2+} concentrations and pH. The results suggest that the rod photoreceptor disks are not discrete, passive sacs but rather comprise an active cellular organelle. The communication between disks may be important for membrane remodeling as well as for providing access to the intradiskal space of the whole outer segment.

INTRODUCTION

Eukaryotic cells contain various membrane organelles, like the endoplasmic reticulum or the Golgi, for carrying out different functions. Vertebrate rod and cone photoreceptors, the cells responsible for visual phototransduction, use a modified cilium (called the outer segment) for the detection of light. Rod photoreceptors mediate vision at low light intensities, whereas cones mediate vision at high light intensities. The rod outer segment is packed with hundreds of membrane sacs (the disks) on the surface of which the initial biochemical reactions of visual transduction take place. The disks are regularly stacked on top of each other with a repeat distance of 300 Å (Blaurock and Wilkins, 1969). Photoreceptor disks are continuously being renewed through formation of new disks at the base of the outer segment, displacement of the disks distally along the length of the outer segment, and eventual detachment and phagocytosis by adjacent pigment epithelial cells (Young, 1967; Anderson and Fisher, 1975). This continuous process of renewal occurs at a massive rate that for amphibian rod photoreceptors amounts to the production of ~3 μm^2 of membrane area per min (Besharse et al., 1977). The morphology of the disks has been investigated in fixed tissue, where rod photoreceptor disks appear to be separate from the plasma membrane and internal to the outer segment (Nilsson, 1965), except from the newly formed disks at the base of the outer segment that are open to the extracellular space (Cohen, 1963). Cone photoreceptor disks on the other hand appear to be open to extracellular space and continuous with the plasma membrane of the outer segment (Cohen, 1968). These results have led to textbook descriptions of the rod disks as discrete and separate from the plasma membrane and each other (Dowling, 1987; Nicholls et al., 2001). Disks have been considered to be passive membrane sacs, whose function is to pack the components of the phototransduction cascade at high concentrations in the outer segment.

We have used fluorescent dyes and single cell imaging to study the properties of disks in living rod photoreceptors. These experiments reveal communication between these disks as well as between disks and extracellular space. Measurements of intradiskal Ca^{2+} concentration and pH find both of them significantly different than intracellular and extracellular Ca^{2+} concentrations and pH, suggesting the presence of dynamic processes operating in the disk membrane.

MATERIALS AND METHODS

Intact rod photoreceptors were isolated from the retinas of dark-adapted larval tiger salamanders (Sullivan Inc., Nashville, TN) or mice by finely chopping the retinas with a razor blade under Ringer's in a petri dish covered with Sylgard elastomer (Dow Corning, Midland, MI). Until the retinas were isolated, all procedures were carried out under infrared illumination with the help of image converters. Afterwards, the retinas were light adapted. Isolated cells were placed in a chamber coated with Concanavalin A for salamander rods and polyornithine for mouse rods (Adler, 1990). For loading photoreceptors with fluorescent dyes, isolated cells or whole retinas were incubated with the dye(s) for 30 to 60 min at room temperature and subsequently washed 3 to 4 times with Ringer's to remove excess dye. The composition of the amphibian Ringer's solution is 110 mM NaCl, 2.5 mM KCl, 1.6 mM $MgCl_2$, 1 mM $CaCl_2$, 5 mM HEPES, 5 mM glucose, pH 7.55. The composition of the mammalian photoreceptor Ringer's solution is (slightly modified from He et al. (2000) and Winkler (1981)): 130 mM NaCl, 5 mM KCl, 0.5 mM $MgCl_2$, 2 mM $CaCl_2$, 25 mM HEPES, 5 mM glucose, pH 7.40, 310-mOsm osmolality. For loading, FM 1-43 and related styryl dyes were used at concentrations of 4 to 32 μM; sulforhodamine 101, thiadicarbocyanine, rhodamine green succinimidyl ester, and tetramethylrhodamine- or Texas Red-labeled dextrans were used

Submitted January 29, 2002, and accepted for publication May 15, 2002.
Address reprint requests to Dr. Yiannis Koutalos University of Colorado Health Sciences Center Department of Physiology and Biophysics, Box C-240 4200 East Ninth Avenue Denver, CO 80262. Tel.: 303-315-4418; Fax: 303-315-8110; E-mail: yiannis.koutalos@uchsc.edu.

0006-3495/02/09/1403/10 $2.00

at 0.2 to 1 mM; whereas the impermeant salts of Fura-2, BTC, and 2′,7′-bis-(2-carboxyethyl)-5(and-6)-carboxyfluorescein (BCECF) were used at 1 mM. The succinimidyl ester is an amino group modifier. BODIPY-labeled phospholipids were used at a concentration of 1 μM. For loading the cytoplasmic space, the acetoxymethyl esters of Fura-2, fluo-3, BCECF, or calcein were used at a concentration of 10 μM. All fluorescent dyes were from Molecular Probes (Eugene, OR).

Imaging experiments were carried out at room temperature on the stage of a Zeiss Axiovert 100 microscope equipped with a SensiCam CCD camera (Cooke Corporation, Auburn Hills, MI), controlled by Intelligent Imaging Innovations (Denver, CO) software. For measuring the fluorescence of different fluorophores, the following combinations of excitation/emission wavelengths (in nm) were used: for FM 1-43, 490/617; for sulforhodamine 101 and the tetramethylrhodamine- or Texas Red-labeled dextrans, 555/617; for thiadicarbocyanine, 640/685; for fluo-3, 490/528. For measurements with ratiometric dyes, the excitation wavelengths were: for Fura-2, 340 and 380 nm; for BTC, 380 and 440 nm; for BCECF, 440 and 495 nm. The emission for all these three ratiometric dyes was monitored at 540 nm. For a ratio R, the Ca^{2+} concentration was calculated as $K_d \times \beta \times (R - R_{min})/(R_{max} - R)$, in which the R_{min} and R_{max} 340/380 and 380/440 ratios and the β parameter (Grynkiewicz et al., 1985) were measured for Fura-2 and BTC in the same imaging setup. For Fura-2, $R_{min} = 0.24$, $R_{max} = 7.10$, $\beta = 16.21$, and $K_d = 224$ nM; for BTC, $R_{min} = 0.02$, $R_{max} = 0.77$, $\beta = 7.37$, and $K_d = 7$ μM. For ultraviolet excitation (340 and 380 nm), there was considerable autofluorescence from rod outer segments that interfered with the Fura-2 and BTC measurements. We corrected for the contribution of autofluorescence by measuring it separately in cells isolated from the same retinas and subtracting it from the fluorescence intensities measured from the cells loaded with the Ca^{2+} dyes. For Ca^{2+} measurements with fluo-3, the F_{min} and F_{max} values were obtained by exposing each cell to 0 Ca^{2+} and Ca^{2+}-Ringer's solutions containing 40 μM ionomycin. The Ca^{2+} concentration was calculated as $K_d \times (F - F_{min})/(F_{max} - F)$, with $K_d = 400$ nM. For converting ratios to pH, the 495/440 ratios for BCECF were measured at four different pHs in the same imaging setup. BCECF was calibrated in three different ways: intracellularly and in vitro using either Ringer's or a high-K^+ solution (110 mM KCl, 1.6 mM $MgCl_2$, 1 mM $CaCl_2$, 5 mM HEPES, 5 mM glucose). For intracellular calibration, the extracellular solutions (same composition as the high-K^+ solutions) contained 10 μM nigericin (Thomas et al., 1979). There was no significant difference between the three calibration curves. BCECF coupled to a 10-kDa dextran was calibrated only with the in vitro solutions, and again, there was no significant difference between the two calibration curves. There was a slight difference between the in vitro pH calibration curves for BCECF and dextran-coupled BCECF. Fig. 1 shows three calibration curves for BCECF: in a high KCl solution (circles), intracellular (triangles), and BCECF coupled to the 10-kDa dextran in a high KCl solution (squares). As expected for that pH range (around the pK of BCECF), the fluorescence ratio changed linearly with pH. The solid line is a least squares fit to the KCl solution points (equation: ratio = $-30.6 + 5.5 \times$ pH) and was not very different from the fit to the intracellular points (ratio = $-26.4 + 4.9 \times$ pH) over the relevant pH range. The dotted line is a least squares fit to the dextran points and is slightly shallower (ratio = $-24.0 + 4.5 \times$ pH) than the others over the relevant pH range.

For measuring the relative loading of dyes of different sizes, we used thiadicarbocyanine as an internal standard. Isolated rod photoreceptors were incubated with a mixture of the dye of interest and thiadicarbocyanine. We measured the loading of a dye in relation to thiadicarbocyanine as the ratio of the dye fluorescence over that of thiadicarbocyanine. To correct for differences in incubating concentration and fluorescence quantum yield, the ratio was normalized over the fluorescence ratio of the incubating mixture.

For fluorescence recovery after photobleaching (FRAP) experiments, an MRC-600 laser scanning confocal microscope (Bio-Rad, Cambridge, MA) equipped with a 5-mW krypton-argon laser was used in a nonconfocal mode. A high intensity of the laser beam was used for bleaching, whereas a lower, nonbleaching intensity was used for scanning and measuring the distribution of fluorescence before and after bleaching. The 488-nm line of the laser was used for experiments with FM 1-43, BODIPY, calcein, and rhodamine green, whereas the 568-nm line was used for experiments with sulforhodamine 101 and Texas Red. After bleaching, images were acquired at regular intervals and were subsequently analyzed with the system software. The fluorescence recovery data were fitted with simple exponentials, providing the fluorescence recovery rates. These rates, along with the size of the cell (length or diameter), were used to obtain the apparent diffusion coefficient for longitudinal or lateral mobility of the fluorophore. The rate r of fluorescence recovery in the longitudinal dimension will be given by the exponent of the first term of the solution to the diffusion equation for a rod insulated at both ends (Carslaw and Jaeger, 1959, p 101, Eq. 6), which for this case is

$$r = \pi^2 \times \frac{D}{L^2} \quad (1)$$

in which D is the longitudinal diffusion coefficient of the fluorophore, and L is the outer segment length. For lateral diffusion, that is diffusion on the plane of the disk membrane or in the intradiskal space, the same Eq. 1 applies with r as the rate of fluorescence recovery in the lateral dimension, D as the lateral diffusion coefficient of the fluorophore, and L as the outer segment diameter (Poo and Cone, 1974).

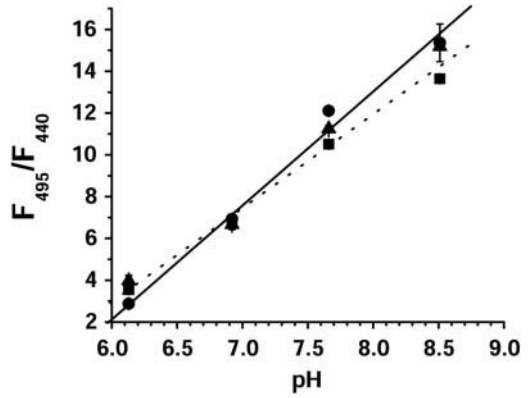

FIGURE 1 Calibration curves for pH measurements for BCECF in a high KCl solution (●), intracellular (▲), and BCECF coupled to the 10-kDa dextran in a high KCl solution (■). The fluorescence emission ratio for excitations at 495 and 440 nm was measured at pHs 6.13, 6.92, 7.66, and 8.51. The straight lines are least squares fit to the BCECF in vitro calibration points (*solid line*) and the BCECF-dextran points (*dotted line*). The standard error bars that do not appear in the graph were smaller than symbol size.

RESULTS

Fig. 2 *a* shows uptake of the fluorescent tracer FM1-43 by a living isolated salamander rod photoreceptor. The fluorescence quantum yield of FM1-43 increases dramatically upon binding to membranes (Betz et al., 1992), allowing the monitoring of the uptake process in the presence of 8 μM FM1-43 in the solution. There was an open zone in the tip area of the outer segment and the concentration of incorporated dye increased with time over the whole length of the outer segment (Fig. 2 *b*). After 30 min, the dye was removed, and with time the fluorescence decreased at the tip but increased in the rest of the outer segment (Fig. 2 *c*),

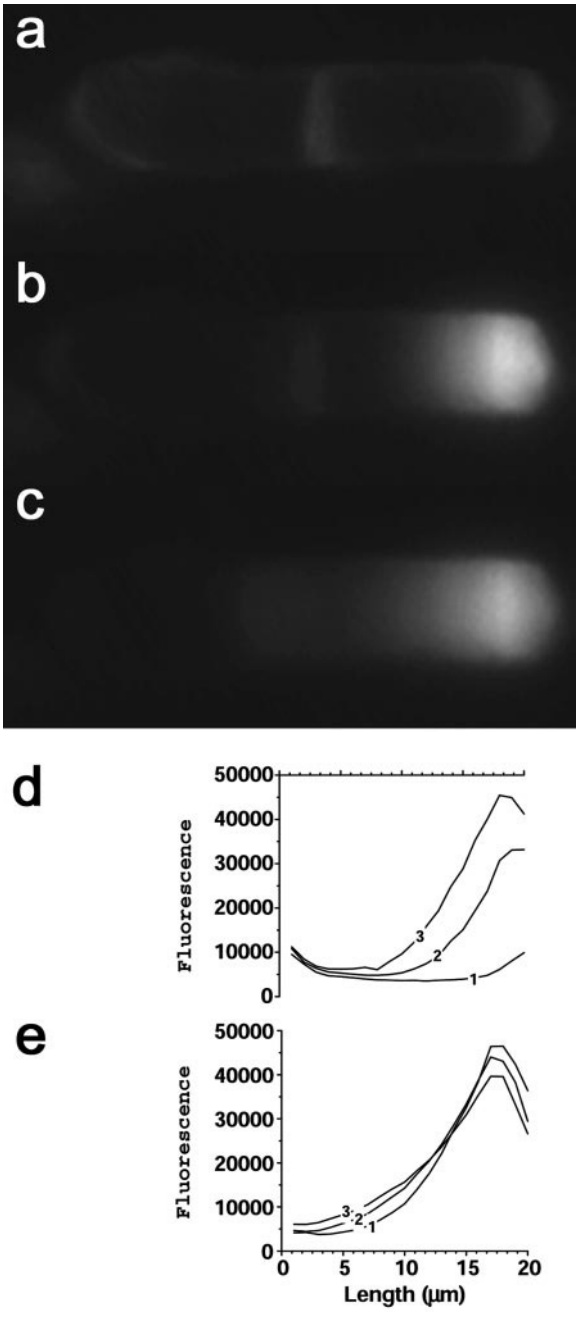

FIGURE 2 Uptake of fluorescent tracers by salamander rod outer segments. (*a*) Isolated rod photoreceptor at the beginning of incubation in the presence of 8 μM FM1-43. (*b*) Thirty minutes after addition, dye has been incorporated into the outer segment through the open zone in the tip area. (*c*) Thirty minutes after the dye has been removed from the extracellular medium, the concentration of dye has decreased in the tip area, but increased in the rest of the outer segment. (*d*) Profiles of fluorescence along the length of the outer segment immediately after addition of FM1-43 in the extracellular medium (*1*), 15 min after addition (*2*), and 30 min after addition (*3*). (*e*) Profiles of fluorescence along the length of the outer segment immediately after removal of FM1-43 from extracellular medium (*1*), 15 min after removal (*2*), and 30 min after removal (*3*).

indicating movement of the incorporated dye from the tip to the base of the outer segment. Fig. 2 *d* shows the changing profiles of fluorescence during the first 30 min in the presence of the dye, indicating a progressive incorporation of the tracer as time went on. Fig. 2 *e* shows the changing distribution of fluorescence during the 30 min after extracellular dye removal. The fluorescence declines in the tip but increases in the base of the outer segment. Because extracellular dye has been removed, these changes indicate movement of the dye from the tip toward the base. FM1-43 does not cross-cell membranes (Henkel et al., 1996), therefore the observed fluorescence cannot be due to dye incorporated in the outer segment cytoplasm. The incorporation of the tracer in the tip can be accounted for by the presence of open disks, as previously observed by staining with Lucifer Yellow (Matsumoto and Besharse, 1985). FM1-43 then initially enters the intradiskal space through these open disks and subsequently moves along the length of the outer segment through a communication pathway between the disks. In separate experiments we have also observed dye incorporation through infrequent and transient disk openings along the length of the outer segment (data not shown). In some experiments the dye was taken up preferentially by the ellipsoid region of the rod, consistent with a process of endocytosis that has been observed before using horseradish peroxidase (Hollyfield and Rayborn, 1987). In these cases, the dye subsequently moved from the ellipsoid to the outer segment, indicating that the communication process is bidirectional. Similar tracer uptake was observed with the related styryl dyes, FM4-64, FM2-10, FM14-68 (Betz et al., 1996), as well as with the polar tracers sulforhodamine 101, thiadicarbocyanine, and a 3-kDa dextran labeled with Texas Red. Confocal sections confirmed that the staining was within the outer segment and not limited to the plasma membrane surface. An important concern is whether the observed spreading of the incorporated tracers is due to abnormal membrane fusion caused by photodamage or the generation of toxic photoproducts. This is unlikely as tracers were found to have spread throughout the rod outer segments after loading in the dark. Also, we have carried out experiments like the one shown in Fig. 2 and examined the spread of the dye from the tip to the rest of the outer segment over a period of 1 h but without the intervening measurements that illuminated the cell. The dye spread in a similar manner as in the experiments in which measurements were carried out at regular intervals, again making photodamage an unlikely cause for the observed spread. It should also be pointed out that the uptake and incorporation of extracellular tracers into the intradiskal compartment was not an artifact of the cell isolation procedure, as similar staining was observed in cells incubated with tracers in whole retinas before dissociation. Fig. 3 shows the comparative loading of rods with sulforhodamine 101 when incubated with the dye after (a) and before (b) dissociation. The loading pattern is the same in both cases (fluorescence

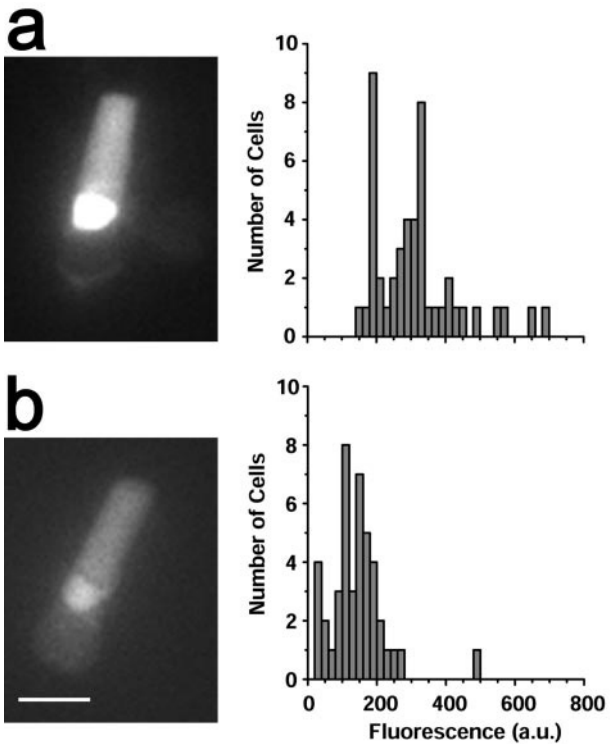

FIGURE 3 Loading of rod outer segments with a polar tracer. Cells were incubated in the dark for 30 to 45 min with 1 mM sulforhodamine in Ringer's. Noninternalized dye was subsequently washed away with Ringer's. Fluorescence was measured within 1 h after the end of incubation. (*a*) Sulforhodamine rod outer segment fluorescence in cells incubated with the tracer after dissociation. The fluorescence image shows a cell loaded in this fashion. (*b*) Sulforhodamine rod outer segment fluorescence in cells incubated with the tracer in whole retinas before dissociation. The fluorescence image shows a cell isolated after incubation with the tracer in a whole retina. Scale bar = 10 μm; the scale is the same for both images.

images), although significantly less dye is incorporated in rod outer segments in the retina (histograms) before dissociation. There was significant incorporation of the tracer in the ellipsoid region of the cell, just below the outer segment, consistent with endocytosis (Hollyfield and Rayborn, 1987). All cells incorporated significant amounts of the dye in the outer segment under both conditions. The lower levels of dye incorporation for cells incubated in the whole retina may be due to the dense packing of the outer segments resulting in lower accessibility for the dye.

We characterized the kinetics of the communication between disks using FRAP. Fig. 4 *a* shows an isolated salamander rod photoreceptor loaded with a 3-kDa dextran coupled to the fluorescent dye Texas Red. This is a polar tracer that is expected to label the intradiskal space. The dye in an area of the outer segment was bleached with a laser beam (Fig. 4 *b*) and the movement of unbleached dye from the rest of the outer segment into the bleached area was followed over time, until the fluorescence in the bleached area recovered after 4.5 min (Fig. 4 *c*). The fluorescence profiles along the length of the outer segment are shown in Fig. 4 *d*, and the recovery kinetics of fluorescence in the bleached part is shown in Fig. 4 *e*. The recovery kinetics was characterized by a rate $r = 0.013\ s^{-1}$, corresponding to an apparent diffusion coefficient $D = 0.76\ \mu m^2\ s^{-1}$, obtained from Eq. 1 for an outer segment length $L = 24\ \mu m$ for this cell.

We also measured the apparent mobilities of other tracers expected to label different outer segment compartments. FM1-43 is expected to label the intradiskal leaflet of the disk membrane bilayer, whereas sulforhodamine 101 is expected to label the intradiskal space. We used calcein-AM to label the cytoplasmic space with calcein; calcein-AM readily crosses the cell membrane and reaches the cytoplasm where esterases cleave the acetoxymethyl ester groups, producing calcein, which remains trapped inside the cell. Finally, we used BODIPY-tagged phospholipids (phosphatidylcholine and phosphatidylethanolamine) to label all membranes. The results are tabulated in Table 1. The apparent diffusion coefficients for longitudinal movement of FM1-43, sulforhodamine 101, and 3- kDa dextran were virtually the same, 0.31 to 0.65 $\mu m^2\ s^{-1}$, indicating that the three tracers were moving through the same process. The cytoplasmic tracer, calcein, was moving much faster with an apparent diffusion coefficient of 42 $\mu m^2\ s^{-1}$, consistent with the cGMP diffusion coefficient of 30 to 60 $\mu m^2\ s^{-1}$ measured with a different approach (Koutalos et al., 1995b). Fluorescent-labeled phospholipids also moved faster than the intradiskal tracers with diffusion coefficients of ~2.3 $\mu m^2\ s^{-1}$. The apparent diffusion coefficients for FM1−43 and the fluorescent-labeled phospholipids were also measured in isolated mouse rod photoreceptors and found to be similar to those for salamander (Table 1).

Fig. 5 shows a schematic representation of the process through which the loading of the intradiskal spaces could take place. In this model, tracers enter the intradiskal space through open disks, present mostly at the tip of rod outer segments, and membrane fusion between neighboring disks

TABLE 1 Apparent diffusion coefficients for different tracers

	Longitudinal diffusion coefficient ($\mu m^2\ s^{-1}$)	Lateral diffusion coefficient ($\mu m^2\ s^{-1}$)
Salamander calcein-AM	42 ± 7 (9)	
Salamander FM1-43	0.53 ± 0.14 (5)	4.7 ± 0.7 (6)
Salamander sulforhodamine 101	0.31 ± 0.08 (4)	6.5 ± 0.8 (8)
Salamander 3 kD dextran	0.65 ± 0.16 (4)	3.0 ± 1.0 (5)
Salamander rhodamine green label	—	0.40 ± 0.06 (8)
Salamander phosphatidylethanolamine	2.3 ± 0.7 (10)	5.1 ± 0.6 (8)
Salamander phosphatidylcholine	2.2 ± 0.4 (9)	3.7 ± 0.5 (5)
Mouse FM1-43	0.78 ± 0.22 (4)	—
Mouse phosphatidylethanolamine	1.6 ± 0.5 (7)	—
Mouse phosphatidylcholine	2.6 ± 0.8 (8)	—

The number of determinations is given in parentheses.

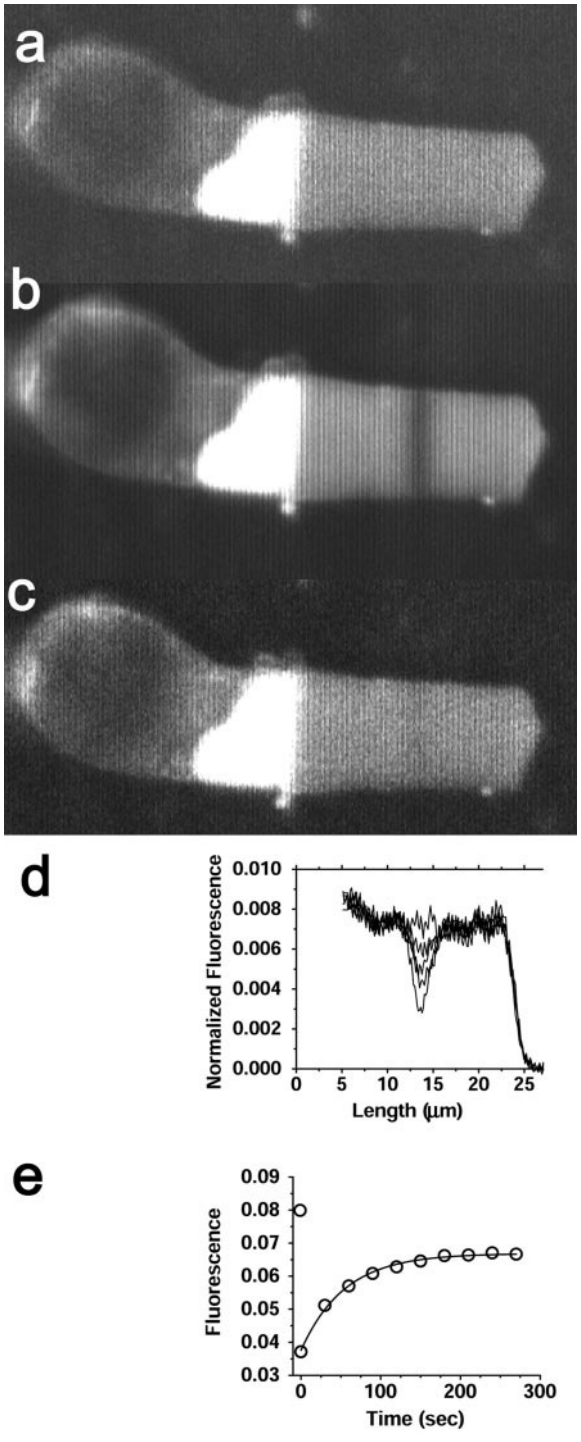

FIGURE 4 FRAP measurements of dye mobility along the length of the rod outer segment. Isolated rods were incubated in the dark for 1 h with 500 μM Texas Red-labeled 3- kDa dextran in Ringer's. Noninternalized dextran was subsequently removed by washing with Ringer's. Measurements were carried out within 2 h after the end of incubation. (*a*) An isolated salamander rod photoreceptor loaded with Texas Red-labeled 3-kDa dextran. (*b*) Immediately after bleaching the dye in an area of the outer segment. (*c*) 4.5 min after the bleach, the fluorescence in the bleached area has recovered as dye from the unbleached areas has moved in. (*d*) Profiles of fluorescence along the length of the outer segment, for the experiment in *a* to *c*. From bottom to top, the shown traces are: immediately after bleach, 0.5 min after, 1 min after, 4.5 min after, initial fluorescence before bleach. (*e*) Kinetics of fluorescence recovery for the bleached area for the experiment in *a* to *c*. The solid line is an exponential least squares fit with rate $r = 0.013\ s^{-1}$. The initial data point is the fluorescence before bleach.

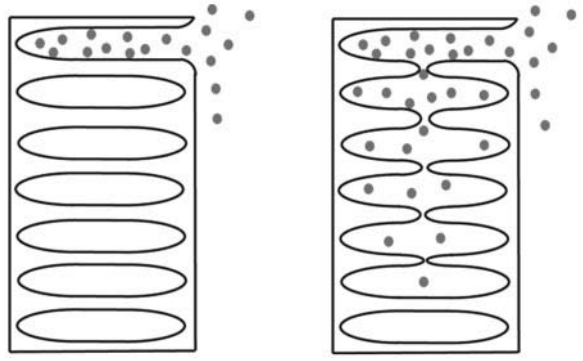

FIGURE 5 Model for the loading of the rod outer segment intradiskal space showing a diagram of a plausible pathway for tracer uptake. Tracers enter the intradiskal space through open disks, present mostly at the tip of rod outer segments (*left*); membrane fusion between neighboring disks allows the exchange of membrane and aqueous phase and the intradiskal tracers move along the length of the outer segment (*right*).

allows the internalized tracers to percolate through the disk stack. We tested this model by comparing the signals of Ca^{2+}- and pH-sensitive dyes incorporated in the cytoplasmic and the intradiskal space. We used the membrane-permeant acetoxymethyl-ester forms of dyes to label the cytoplasm and the membrane-impermeant salts to label the intradiskal space. Fig. 6 shows the results obtained by loading rod photoreceptors with the pH-sensitive dye BCECF. Fig. 6, *a* and *b* show fluorescence images of rod photoreceptors loaded with BCECF-AM and BCECF, respectively. In the rod outer segment loaded with the impermeant salt of BCECF (Fig. 6 *b*), there is a band of bright staining (arrow) that reflects high dye concentration, likely to have been incorporated in disks open to extracellular space. For this rod outer segment, the pH in the band was 7.30, whereas the pH in the rest of the outer segment (diffuse staining) was 7.11. Overall, the cytoplasmic pH was 7.29 ± 0.02 ($n = 27$) in good agreement with ^{31}P-nuclear magnetic resonance measurements (Apte et al., 1993), whereas intradiskal BCECF reported a pH of 6.50 ± 0.07 ($n = 35$) (Fig. 6 *c*). On the other hand, BCECF coupled to a 10-kDa dextran reported an intradiskal pH of 7.21 ± 0.02 ($n = 17$), suggesting limited access of high molecular weight molecules through the communication pathway between the disks: the 10-kDa dextran is limited to intradiskal spaces that are in close communication with extracellular space, and therefore have a higher pH, closer to the extracellular pH of 7.55. Consistent with this interpretation, areas staining brightly with free BCECF and reflecting high dye concentrations incorporated in open disks, had higher pH

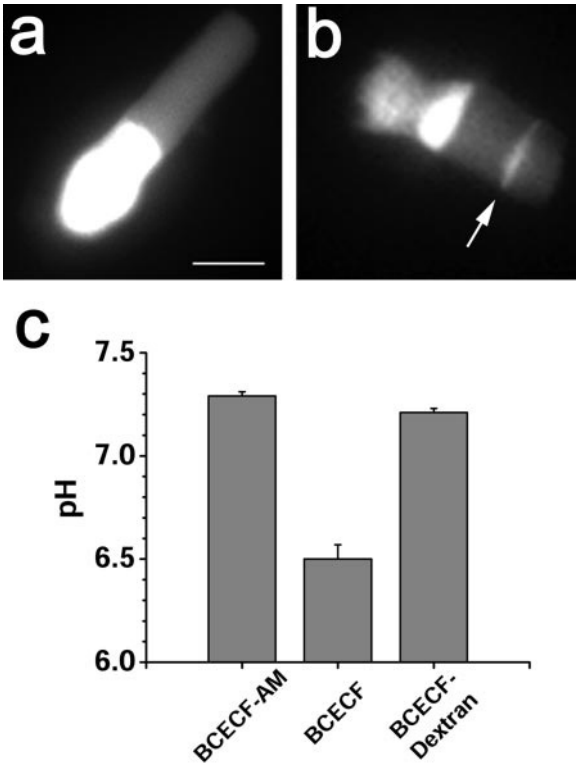

FIGURE 6 Rod outer segment pH values measured by different tracers in distinct compartments: (*a*) Fluorescence image (excitation 495 nm) of an isolated salamander rod loaded with BCECF acetoxymethyl ester (BCECF-AM). Isolated cells were incubated in the dark for 30 min with 10 μM BCECF-AM in Ringer's. Excess dye was subsequently removed by washing with Ringer's. Measurements were carried out within 2 h after the end of incubation. Scale bar = 10 μm. (*b*) Fluorescence image of an isolated salamander rod loaded with free BCECF (excitation 495 nm). Whole retinas were incubated in the dark for 1 h with 1 mM BCECF in Ringer's. Noninternalized dye was subsequently removed by washing with Ringer's and isolated cells were obtained by dissociation. Measurements were carried out within 2 h after the end of incubation. Scale is the same as in *a*. This particular cell showed a band of bright staining in the outer segment (*arrow*) indicating high dye concentration. The pH in the band was 7.30, whereas in the rest of the outer segment (diffuse staining) was 7.11. (*c*) Collected pH data: BCECF-AM produces BCECF in the cytoplasm and reports a cytoplasmic pH of 7.29 $\pm$ 0.02 (n = 27); free BCECF enters the intradiskal space and reports a pH of 6.50 $\pm$ 0.07 (n = 35); BCECF coupled to a 10-kDa dextran has limited access to intradiskal space and reports a pH of 7.21 $\pm$ 0.02 (n = 17). Error bars represent standard errors.

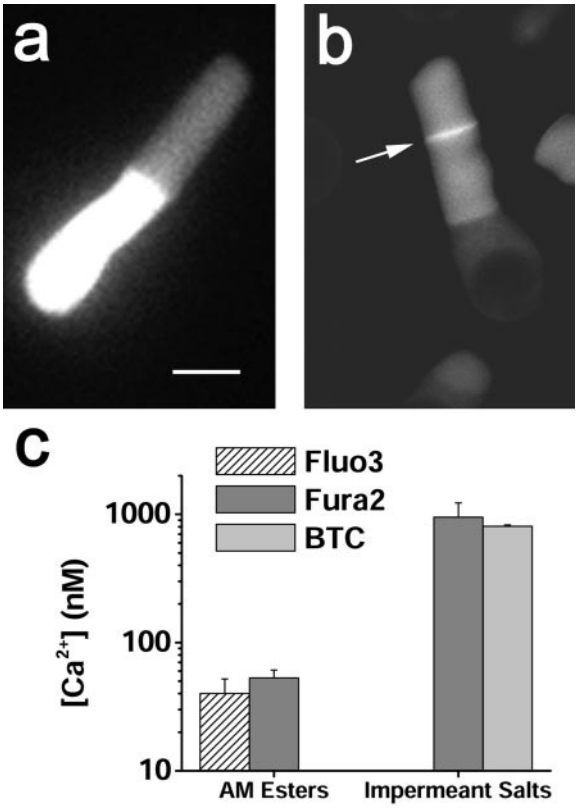

FIGURE 7 Rod outer segment free Ca^{2+} concentrations measured by different tracers in distinct compartments. (*a*) Fluorescence image (excitation 380 nm) of an isolated salamander rod loaded with Fura-2 acetoxymethyl ester (AM). Isolated cells were incubated in the dark for 30 min with 10 μM Fura-2-AM in Ringer's. Excess dye was subsequently removed by washing with Ringer's. Measurements were carried out within 2 h after the end of incubation. Scale bar = 10 μm. (*b*) Fluorescence image (excitation 440 nm) of an isolated salamander rod loaded with free BTC. Whole retinas were incubated in the dark for 1 h with 1 mM BTC in Ringer's. Noninternalized dye was subsequently removed by washing with Ringer's and isolated cells were obtained by dissociation. Measurements were carried out within 2 h after the end of incubation. Scale is the same as in *a*. This particular cell showed a band of bright staining in the outer segment (*arrow*), indicating high dye concentration. The Ca^{2+} concentration in the band was ~2.7 μM, whereas in the rest of the outer segment (diffuse staining) was ~0.8 μM. (*c*) Ca^{2+} concentrations reported by the dyes from different compartments. Fluo-3 and Fura-2 acetoxymethyl (AM) esters produce free fluo-3 and Fura-2 in the cytoplasm and report cytoplasmic Ca^{2+} concentrations of 40 $\pm$ 12 (n = 7) and 53 $\pm$ 8 nM (n = 40), respectively; free Fura-2 and free BTC enter the intradiskal space and report intradiskal Ca^{2+} concentrations of 0.95 $\pm$ 0.27 (n = 31) and 0.81 $\pm$ 0.02 μM (n = 57), respectively. Error bars represent standard errors.

7.38 $\pm$ 0.10 (n = 10), reflecting the close communication with extracellular space. The pH values reported here are quite reliable: they are based on extensive BCECF calibrations that were carried out under various conditions, all of which gave consistent results (Fig. 1).

Fig. 7 shows the results obtained with the Ca^{2+}-sensitive dyes Fura-2, fluo-3, and BTC. Fig. 7, *a* and *b* shows fluorescence images of rods loaded with Fura-2-AM and the impermeant salt of BTC, respectively. In the rod outer segment loaded with the impermeant salt of BTC (Fig. 7 *b*), there is a band of bright staining (arrow) that reflects high dye concentration, again likely to have been incorporated in disks open to extracellular space. For this rod outer segment, the Ca^{2+} concentration in the band was ~2.7 μM, whereas the concentration in the rest of the outer segment (diffuse staining) was ~0.8 μM. Overall, the free Ca^{2+} concentration in the cytoplasm was ~50 nM, in good agreement with the concentration measured in rod outer segments after bleaching (Gray-Keller and Detwiler, 1994; Sampath

et al., 1998), whereas inside the disks was ~1 μM (Fig. 7 *c*). For the few cells that showed localized staining in the outer segments with the impermeant salts of the dyes, the Ca^{2+} concentration in the bands of high dye concentration was higher than in the outer segment areas of diffuse staining. It is important to note that the Ca^{2+} concentrations reported here reflect approximate values as the Fura-2 and BTC dye calibrations were carried out in vitro, and the K_ds used were obtained from Molecular Probes. Nevertheless, because for Fura-2 the same calibration was used, the difference between the cytoplasmic and intradiskal values does not depend on the calibration, suggesting that the permeant and impermeant forms of the dyes occupy different compartments.

The ability of 3-kDa dextran in contrast to the known inability of rhodopsin to pass from disk to disk, gave rise to the question whether there is a size filter in the interdiskal communication pathway. We addressed this question by examining the loading of dyes of different sizes in rod outer segments. Because the loading was quite variable from cell to cell, we used a polar tracer, thiadicarbocyanine, as an internal standard. This fluorophore, with a molecular weight of 776, loads well in the intradiskal space, and its fluorescence excitation and emission spectra allow it to be used for double labeling. Fig. 8, *a* and *b* show the loading of rod photoreceptors with a 3-kDa dextran and a 10-kDa lipophilic dextran, respectively. Fig. 8 *a* is fairly representative of the loading pattern for the 3-kDa dextran or sulforhodamine (see also Fig. 3). The loading pattern for the 10-kDa lipophilic dextran was quite variable. The cell in Fig. 8 *b* shows essentially no loading, apart from the tip area where loading is quite pronounced. Several cells showed essentially no loading, whereas others showed a significant amount. Fig. 8 *c* shows the relative loading of rod outer segments with sulforhodamine (molecular weight = 607), and three dextrans, 3-kDa, 10-kDa polar, and 10-kDa lipophilic. There was almost no loading with the 10-kDa polar dextran, whereas, as mentioned above, the loading with the 10-kDa lipophilic dextran was quite variable hence the large error bar. These data suggest that molecules smaller than 3 kDa pass readily through the interdiskal communication pathway, but molecules larger than 10 kDa do not. This interpretation is also in agreement with the higher pH reported by BCECF coupled to a 10-kDa dextran (Fig. 6 *c*).

Subsequently, we examined the diffusion of tracers in the intradiskal space. Fig. 9 *a* shows a salamander rod loaded with FM1-43. The outer segment FM1-43 fluorescence was bleached at a spot with the laser (Fig. 9 *b*), and the lateral movement of unbleached dye into the bleached area was followed over time, until the fluorescence in the spot equilibrated laterally after 20 s (Fig. 9 *c*). The fluorescence profiles for Fig. 9, *a* to *c*, are shown in Fig. 9 *d*, and the recovery kinetics of the fluorescence in the bleached spot is shown in Fig. 9 *e*. Fluorescence recovery was characterized

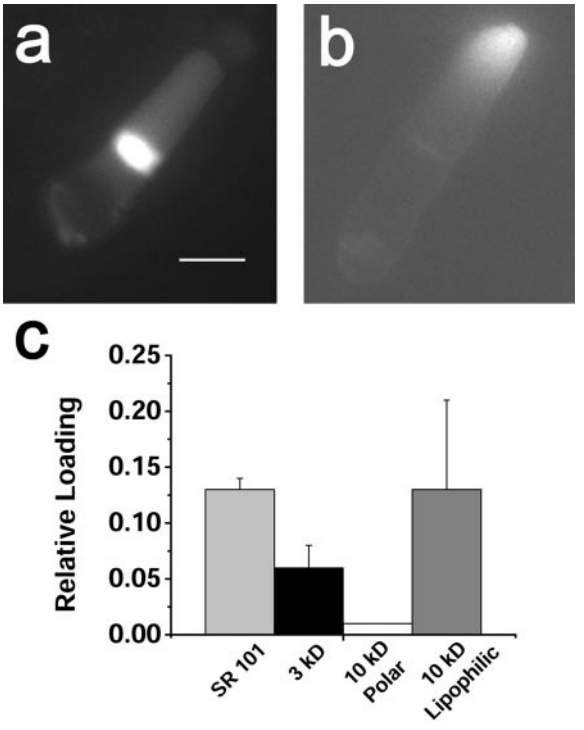

FIGURE 8 Differences in the loading of rod outer segments with dyes of different sizes suggest the presence of a size filter in the communication pathway between disks. Isolated cells were incubated in the dark for 1 h with 200 μM thiadicarbocyanine and 500 μM of another tracer in Ringer's. Noninternalized dyes were subsequently removed by washing with Ringer's. Measurements were carried out within 2 h after the end of incubation. (*a*) Texas Red fluorescence of an isolated rod photoreceptor loaded with thiadicarbocyanine and a Texas Red-labeled 3-kDa dextran. Scale bar = 10 μm. (*b*) Tetramethylrhodamine fluorescence of an isolated rod photoreceptor loaded with thiadicarbocyanine and a tetramethylrhodamine-labeled 10-kDa lipophilic dextran. Scale is the same as in *a*. The cell shows essentially no loading, apart from the tip area where loading is quite pronounced. (*c*) Relative loading of different tracers in rod outer segments. Thiadiacarbocyanine loading corresponds to 1.0. SR 101 stands for sulforhodamine 101. Error bars represent standard errors.

by a rate $r = 0.24\ s^{-1}$, corresponding to an apparent diffusion coefficient $D = 4.8\ \mu m^2\ s^{-1}$, obtained from Eq. 1 for an outer segment diameter $d = 14\ \mu m$ for this cell. The apparent diffusion coefficients for lateral movement of FM1-43, sulforhodamine 101, the 3-kDa dextran, and the fluorescent-labeled phospholipids are shown in Table 1. For comparison, we also measured the apparent diffusion coefficient of proteins labeled with rhodamine green succinimidyl ester. This modifier should label protein amino groups with rhodamine green. The apparent diffusion coefficient was $0.4\ \mu m^2\ s^{-1}$, consistent with the diffusion coefficient of rhodopsin (Poo and Cone, 1974; Liebman and Entine, 1974), which constitutes the major protein in the rod outer segment. The rhodamine green-labeled proteins moved laterally, but not longitudinally, consistent with the previous observation that rhodopsin does not move from disk to disk (Liebman and Entine, 1974). Lateral equilibration, perpen-

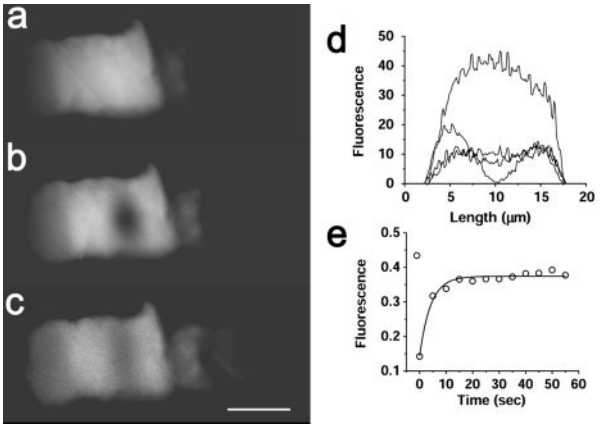

FIGURE 9 Diffusion of tracers inside disks. Isolated rods were incubated in the dark for 1 h with 16 to 32 μM FM1-43 in Ringer's. Noninternalized dye was subsequently removed by washing with Ringer's. Measurements were carried out within 2 h after the end of incubation. (*a*) An isolated salamander rod photoreceptor loaded with FM1-43. (*b*) Immediately after bleaching the dye in a spot of the outer segment. (*c*) Twenty seconds after the bleach, the fluorescence in the bleached spot has recovered as the dye has equilibrated within disks. Scale bar = 10 μm. (*d*) Profiles of fluorescence along a diameter of the outer segment, for the experiment in *a* to *c*. From bottom to top, the shown traces are: immediately after bleach, 5 s after, 50 s after, initial fluorescence before bleach. (*e*) Kinetics of fluorescence recovery for the bleached spot for the experiment in *a* to *c*. The solid line is an exponential least squares fit with rate $r = 0.24$ s^{-1}. The initial data point is the fluorescence before bleach.

dicular to the axis of the rod outer segment, was observed with all tracers, indicating that the stacked-disk structure of the rod outer segment had not been disrupted.

DISCUSSION

The results presented above indicate communication between rod photoreceptor outer segment disks. An important concern is whether the observed communication is an artifact of the cell isolation procedures. This is unlikely, because similar uptake and incorporation of extracellular tracers into the intradiskal compartment was observed when cells were incubated with tracers in whole retinas before dissociation. Moreover, when a tracer was destroyed in FRAP experiments, as the one in Fig. 9, it subsequently equilibrated laterally, indicating that the stack of disks in the rod outer segment had not been disrupted. Electron microscopic studies have also shown that rod cells dissociated from salamander retina retain their stack of membranous disks in culture (Townes-Anderson et al., 1985). A related concern may be that there is a large body of evidence suggesting that rod outer segment disks are discrete and separate from each other and the plasma membrane (Nilsson, 1965; Cohen, 1963, 1968). However, most of these studies have been carried out with fixed rod outer segments and may have missed a transient, dynamic process. Communication between intradiskal and extracellular space has been observed in the tips of *Xenopus laevis* rod outer segments by staining with Lucifer Yellow (Matsumoto and Besharse, 1985). Also, some sort of communication between disks could have been inferred on the basis of the observation that radioactively labeled lipids incorporated in rod outer segments show diffuse distribution, leading to the conclusion that "membrane renewal by molecular replacement is more rapid for lipid than it is for protein" (Bibb and Young, 1974a,b). An observation potentially contradictory to the results reported here is that Procion Yellow, injected into the vitreous cavity of eyes of living animals, stains only the new-forming basal disks of rod outer segments (Laties et al., 1976). The stained disks gradually move toward the pigment epithelium, and a few days after the injection, a length of unstained outer segment separates the stained disks from the base of the outer segment (Laties et al., 1976). A possible reconciliation of these observations with the ones reported here is that Procion Yellow binds covalently to subcellular organelles and proteins with the probable site of attachment being the amino group (Flanagan et al., 1974). In this case, the observed Procion Yellow staining of the basal disks would be due to covalent binding to proteins (mostly rhodopsin), and the result would be consistent with the one reported here for labeling with rhodamine green succinimidyl ester. The result obtained with the rhodamine green label is in agreement with the observation that the visual pigment, rhodopsin, does not move from disk to disk (Liebman and Entine, 1974) and consistent with the finding that the communication pathway has a size filter, which allows the passage of molecules smaller than 3 kDa but not larger than 10 kDa.

The interdiskal communication process reported here involves the exchange of both aqueous and membrane tracers. Thus, although the mechanism underlying this communication is not clear, it involves the exchange of both aqueous and membrane phase and therefore it is likely to involve some form of membrane fusion. Membrane fusion has been observed with isolated disk membranes in vitro (Boesze-Battaglia and Yeagle, 1992), and peripherin/rds, a disk membrane protein, has been implicated in disk membrane fusion (Boesze-Battaglia et al., 1998). Paracrystalline inclusions that have been observed in freeze-fracture micrographs from rod outer segments (Corless and Costello, 1981) may also be part of a communication pathway between disks. From the mobility measurements shown in Table 1, we can estimate the area of the aqueous conduits constituting the communication pathway between disks. If F_A is the fraction of this area and F_V the fraction of rod outer segment volume available for aqueous tracer diffusion, then the ratio $f = D_{long}/D_{lat}$ of longitudinal and lateral diffusion coefficients is given by $f = F_A/[F_V\ (1 - F_V + F_A)]$ (Koutalos et al., 1995a). The cytoplasmic volume is 50% of outer segment volume, because the thickness of each disk is approximately one-half the repeat distance (Korenbrot et al., 1973, Table 1). The available volume

within a disk, F_V, has been estimated to be ~25% of the cytoplasmic volume (Cohen, 1971), a value consistent with an intradiskal space thickness of 40 Å and a disk membrane thickness of 55 Å (Blaurock and Wilkins, 1969). Therefore, $F_V \sim 0.13$. For the 3-kDa dextran, its longitudinal mobility is ~5× lower than its lateral mobility (Table 1), so $f \sim 0.2$, resulting in $F_A \sim 0.023$. That is, the aqueous conduits of the communication pathway occupy ~2.3% of the disk area. The paracrystalline inclusions that may be related to this communication have been estimated to occupy 1% of outer segment volume (Corless and Costello, 1981).

Phospholipids move much faster than polar tracers along the length of the outer segment (Table 1), a property that may reflect the significant occurrence of hemifusion without the opening of an aqueous pore (Kemble et al., 1994), that is, a transition state that would allow the movement of phospholipids but not that of FM1-43, dextran, or sulforhodamine. Another possible mechanism that could explain the faster movement of phospholipids would be the participation of transfer proteins (Dudley and Anderson, 1978). Phospholipids have been known to equilibrate rapidly, within hours, along the length of the rod outer segment (Bibb and Young, 1974a,b; Basinger and Hoffman, 1976; Wetzel and Besharse, 1994), and the observed communication between the disks can account for this rapid equilibration. In terms of lateral mobility, the phospholipid and FM1-43 diffusion coefficients were 4 to 5 $\mu m^2\ s^{-1}$, in agreement with lipid diffusion in membranes (Scandella et al., 1972).

The experiments have also provided information about the properties of the intradiskal space. The apparent diffusion coefficients for sulforhodamine 101 and the 3-kDa dextran, 6.5 $\mu m^2\ s^{-1}$, and 3 $\mu m^2\ s^{-1}$ respectively, were almost 100× less than the predicted diffusion coefficients in solution (Kushmerick and Podolsky, 1969) suggesting that diffusion in the intradiskal space is highly hindered. In addition, the intradiskal pH value of 6.5 is similar to that measured for the Golgi (Kim et al., 1996; Llopis et al., 1998). On the other hand, the intradiskal Ca^{2+} concentration of 1 μM is much lower than the 310 ± 46 μM reported for Golgi (Pinton et al., 1998). The total Ca^{2+} content of rod outer segments is in the order of 1 to 3 Ca^{2+} ions per rhodopsin, and most of it appears to be sequestered inside the disks (Schnetkamp, 1979; Fain and Schröder, 1985). From Ca^{2+} titrations of isolated bovine rod outer segments using atomic absorption measurements, Schnetkamp (1979) estimated that intradiskal Ca^{2+} binding sites have a capacity of 8 to 9 Ca^{2+} per rhodopsin and are at equilibrium with an intradiskal free Ca^{2+} concentration of 15 to 25 μM. This value is in somewhat reasonable agreement with the 1 μM value reported here considering the differences in techniques, calibrations, and species (bovine versus salamander). Of course, the pH and Ca^{2+} concentrations reported here are for bleached cells, and dark-adapted cells may differ. This is a particularly relevant point as disks appear to be nearly impermeable to Ca^{2+} under physiological conditions in darkness (Fain and Schröder, 1985), but may release Ca^{2+} in bright light (Fain and Schröder, 1990). The intradiskal H^+ and Ca^{2+} concentrations reported here are significantly different from both cytoplasmic and extracellular concentrations, perhaps indicating the presence of transport processes that maintain these ionic gradients. We have no direct evidence for the presence of significant transport mechanisms operating on the disk membrane. It could very well be the case that the intradiskal Ca^{2+} concentration is the result of a slow communication of the intradiskal with extracellular space via the newly forming open disks at the base and the open disks at the tip, coupled perhaps with a slow transport process on the disk membrane.

The measurements and comparisons of the pH and Ca^{2+} concentrations of cytoplasmic and intradiskal space have used the membrane-permeant acetoxymethyl ester (AM) forms of different dyes. Although these compounds may also enter the intradiskal space, we consider it unlikely that they are converted into the optically active forms inside the intradiskal space. The reasons are: the calcein and fluo-3 released from the AM forms diffuse with the diffusion coefficient of a cytoplasmic tracer (present study; Nakatani et al., 2002); the Fura-2 and fluo-3 released from the AM forms report a Ca^{2+} concentration consistent with the cytoplasmic value in bleached cells; the BCECF released from the AM form reports a pH consistent with cytoplasmic pH.

In summary, the photoreceptor disks comprise an active organelle, similar to other membrane organelles like the Golgi or endoplasmic reticulum. There is dynamic communication between disks as well as between disks and extracellular space, allowing the exchange of membrane and aqueous molecules. This pathway could account for the rapid equilibration of certain phospholipids along the length of the rod outer segment and be relevant for the extensive remodeling of outer segment membranes known to occur (Giusto et al., 2000). It could also allow for the transport of molecules along the length of the outer segment through the intradiskal space.

We thank Dr. A. Zweifach for advice, discussions, and encouragement, and a critical reading of the manuscript, Drs. W.J. Betz and J. Angleson for helpful discussions and suggestions, and S. Fadul for assistance with the use of the laser scanning confocal microscope. This work was supported by National Institutes of Health grant EY11351 (to Y.K.).

REFERENCES

Adler, R. 1990. Preparation, enrichment, and growth of purified cultures of neurons and photoreceptors from chick embryos and from normal and mutant mice. *Methods Neurosci.* 2:134–150.

Anderson, D. H., and S. K. Fisher. 1975. Disk shedding in rodlike and conelike photoreceptors of tree squirrels. *Science.* 187:953–955.

Apte, D. V., T. G. Ebrey, and M. J. Dawson. 1993. Decreased energy requirement of toad retina during light adaptation as demonstrated by ^{31}P nuclear magnetic resonance. *J. Physiol.* 464:291–306.

Basinger, S., and R. Hoffman. 1976. Phosphatidylcholine metabolism in the frog rod photoreceptor. *Exp. Eye Res.* 23:117–126.

Besharse, J. C., J. G. Hollyfield, and M. E. Rayborn. 1977. Turnover of rod photoreceptor outer segments: II. Membrane addition and loss in relationship to light. *J. Cell Biol.* 75:507–527.

Betz, W. J., F. Mao, and G. S. Bewick. 1992. Activity-dependent fluorescent staining and destaining of living vertebrate motor nerve terminals. *J. Neurosci.* 12:363–375.

Betz, W. J., F. Mao, and C. B. Smith. 1996. Imaging exocytosis and endocytosis. *Curr. Opin. Neurobiol.* 6:365–371.

Bibb, C., and R. W. Young. 1974a. Renewal of fatty acids in the membranes of visual cell outer segments. *J. Cell Biol.* 61:327–343.

Bibb, C., and R. W. Young. 1974b. Renewal of glycerol in the visual cells and pigment epithelium of the frog retina. *J. Cell Biol.* 62:378–389.

Blaurock, A. E., and M. H. F. Wilkins. 1969. Structure of frog photoreceptor membranes. *Nature.* 223:906–909.

Boesze-Battaglia, K., O. P. Lamba, A. A. Napoli, S. Sinha, and Y. Guo. 1998. Fusion between rod outer segment membranes and model membranes: a role for photoreceptor peripherin/rds. *Biochemistry.* 37: 9477–9487.

Boesze-Battaglia, K., and P. L. Yeagle. 1992. Rod outer segment disc membranes are capable of fusion. *Invest. Ophthalmol. Vis. Sci.* 33: 484–493.

Carslaw, H. S., and J. C. Jaeger. 1959. Conduction of Heat in Solids, 2nd Ed, Equation 6. Oxford University Press, New York. 101.

Cohen, A. I. 1963. Vertebrate retinal cells and their organization. *Biol. Rev.* 38:427–459.

Cohen, A. I. 1968. New evidence supporting the linkage to extracellular space of outer segment saccules of frog cones but not rods. *J. Cell Biol.* 37:424–444.

Cohen, A. I. 1971. Electron microscope observations on form changes in photoreceptor outer segments and their saccules in response to osmotic stress. *J. Cell Biol.* 48:547–565.

Corless, J. M., and M. J. Costello. 1981. Paracrystalline inclusions associated with the disk membranes of frog retinal rod outer segments. *Exp. Eye Res.* 32:217–228.

Dowling, J. E. 1987. The Retina: An Approachable Part of the Brain. Belknap Press, Cambridge, MA. 194.

Dudley, P. A., and R. E. Anderson, R. E. 1978. Phospholipid transfer protein from bovine retina with high activity toward retinal rod disc membranes. *FEBS Lett.* 95:57–60.

Fain, G. L., and W. H. Schröder. 1985. Calcium content and calcium exchange in dark-adapted toad rods. *J. Physiol.* 368:641–665.

Fain, G. L., and W. H. Schröder. 1990. Light-induced calcium release and reuptake in toad rods. *J. Neurosci.* 10:2238–2249.

Flanagan, M. T., T. R. Hesketh, and S.-H. Chung. 1974. Procion yellow M-4RS binding to neuronal membranes. *J. Histochem. Cytochem.* 22: 952–961. N. M.

Giusto, N. M., S. J. Pasquare, G. A. Salvador, P. I. Castagnet, M. E. Roque, and M. G. Ilincheta de Boscher. 2000. Lipid metabolism in vertebrate retinal rod outer segments. *Progr. Lipid Res.* 39:315–391.

Gray-Keller, M., and P. B. Detwiler. 1994. The calcium feedback signal in the phototransduction cascade of vertebrate rods. *Neuron.* 13:849–861.

Grynkiewicz, G., M. Poenie, and R. Y. Tsien. 1985. A new generation of Ca^{2+} indicators with greatly improved fluorescence properties. *J. Biol. Chem.* 260:3440–3450.

He, L., A. T. Poblenz, C. J. Medrano, and D. A. Fox. 2000. Lead and calcium produce rod photoreceptor cell apoptosis by opening the mitochondrial permeability transition pore. *J. Biol. Chem.* 275:12175–12184.

Henkel, A. W., J. Lübke, and W. J. Betz. 1996. FM1–43 dye ultrastructural localization in and release from frog motor nerve terminals. *Proc. Natl. Acad. Sci. U.S.A.* 93:1918–1923.

Hollyfield, J. G., and M. E. Rayborn. 1987. Endocytosis in the inner segment of rod photoreceptors: analysis of *Xenopus laevis* retinas using horseradish peroxidase. *Exp. Eye Res.* 45:703–719.

Kemble, G. W., T. Danieli, and J. M. White. 1994. Lipid-anchored influenza hemagglutinin promotes hemifusion, not complete fusion. *Cell.* 76:383–391.

Kim. J. H., C. A. Lingwood, D. B. Williams, W. Furuya, M. F. Manolson, and S. Grinstein. 1996. Dynamic measurement of the pH of the Golgi complex in living cells using retrograde transport of the verotoxin receptor. *J. Cell Biol.* 134:1387–1399.

Korenbrot, J. I., D. T. Brown, and R. A. Cone. 1973. Membrane characteristics and osmotic behavior of isolated rod outer segments. *J. Cell Biol.* 56:389–398.

Koutalos, Y., R. L. Brown, J. W. Karpen, and K.-W. Yau. 1995a. Diffusion coefficient of the cyclic GMP analog 8-(fluoresceinyl)thioguanosine 3′,5′ cyclic monophosphate in the salamander rod outer segment. *Biophys. J.* 69:2163–2167.

Koutalos, Y., K. Nakatani, and K.-W. Yau. 1995b. Cyclic GMP diffusion coefficient in rod photoreceptor outer segments. *Biophys. J.* 68:373–382.

Kushmerick, M. J., and R. J. Podolsky. 1969. Ionic mobility in muscle cells. *Science.* 166:1297–1298.

Laties, A. M., D. Bok, and P. Liebman. 1976. Procion yellow: a marker dye for outer segment disc patency and for rod renewal. *Exp. Eye Res.* 23:139–148.

Liebman, P. A., and G. Entine. 1974. Lateral diffusion of visual pigment in photoreceptor disk membranes. *Science.* 185:457–459.

Llopis, J., J. M. McCaffery, A. Miyawaki, M. Farquhar, and R. Y. Tsien. 1998. Measurement of cytosolic, mitochondrial, and Golgi pH in single living cells with green fluorescent proteins. *Proc. Natl. Acad. Sci. U.S.A.* 95:6803–6808.

Matsumoto, B., and J. C. Besharse. 1985. Light and temperature modulate staining of the rod outer segment distal tips with Lucifer Yellow. *Invest. Ophthalmol. Vis. Sci.* 26:628–635.

Nakatani, K., C. Chen, and Y. Koutalos . 2002. Calcium diffusion coefficient in rod photoreceptor outer segments. *Biophys. J.* 82, 728–739.

Nicholls, J. G., A. R. Martin, B. G. Wallace, and P. A. Fuchs. 2001. From Neuron to Brain, 4th Ed. Sinauer Associates, Sunderland, MA. 383.

Nilsson, S. E. G. 1965. The ultrastructure of the receptor outer segments in the retina of the leopard frog (*Rana pipiens*). *J. Ultrastruct. Res.* 12: 207–231.

Pinton, P., T. Pozzan, and R. Rizzuto. 1998. The Golgi apparatus is an inositol 1,4,5-trisphosphate-sensitive Ca^{2+} store, with functional properties distinct from those of the endoplasmic reticulum. *EMBO J.* 17: 5298–5308.

Poo, M., and R. A. Cone. 1974. Lateral diffusion of rhodopsin in the photoreceptor membrane. *Nature.* 274:438–441.

Sampath, A. P., H. R. Matthews, M. C. Cornwall, and G. L. Fain. 1998. Bleached pigment produces a maintained decrease in outer segment Ca^{2+} in salamander rods. *J. Gen. Physiol.* 111:53–64.

Scandella, C. J., P. Devaux, and H. M. Mc. 1972. Rapid lateral diffusion of phospholipids in rabbit sarcoplasmic reticulum. *Proc. Natl. Acad. Sci. U.S.A.* 69:2056–2060.

Schnetkamp, P. P. M. 1979. Calcium translocation and storage of isolated intact cattle rod outer segments in darkness. *Biochim. Biophys. Acta.* 554:441–459.

Thomas, J. A., R. N. Buchsbaum, A. Zimniak, and E. Racker. 1979. Intracellular pH measurements in Ehrlich ascites tumor cells utilizing spectroscopic probes generated in situ. *Biochemistry.* 18:2210–2218.

Townes-Anderson, E., P. R. MacLeish, and E. Raviola. 1985. Rod cells dissociated from mature salamander retina: ultrastructure and uptake of horseradish peroxidase. *J. Cell Biol.* 100:175–188.

Wetzel, M. G., and J. C. Besharse. 1994. Transport of phosphatidylcholine to *Xenopus* photoreceptor rod outer segments in the presence of tunicamycin. *J. Neurocytol.* 23:333–342.

Winkler, B. S. 1981. Glycolytic and oxidative metabolism in relation to retinal function. *J. Gen. Physiol.* 77:667–692.

Young, R. W. 1967. The renewal of photoreceptor cell outer segments. *J. Cell Biol.* 33:61–72.